Supporting Information to Accompany:

Me_3P Complexes of p-Block Lewis Acids $SnCl_4$, $SnCl_3^+$ and $SnCl_2^{2+}$

Elizabeth MacDonald,[a] Lauren Doyle,[a] Saurabh S. Chitnis,[b] Ulrike Werner-Zwanziger,[a] Neil Burford[b*] and Andreas Decken,[c]

[a] Department of Chemistry, Dalhousie University, Halifax, NS, B3H 4J3, Canada

[b] Department of Chemistry, University of Victoria, Victoria, BC, V8W 3V6, Canada

[c] Department of Chemistry, University of New Brunswick, Fredericton, NB, E3A 6E2, Canada

---

General Experimental Procedures:

Small scale reactions were carried out in an IT System One Manual glovebox with an inert N_2 atmosphere containing less than 10 ppm of oxygen and less than 5 ppm water. Initial reactions were done in 14.8 mL glass vials with Teflon-lined caps and larger scale reactions used 100 mL round schlenk glassware with Teflon needle valves and ground glass joint stoppers. All glassware was stored overnight in an oven at 170 °C and pumped into the glove-box while hot, or was flame-dried under vacuum prior to use.

Solvents were deoxygenated by sparging with N_2(g) for 45 mins and collected by a double column MBraun solvent purification system which had solvent pass over one column packed with alumina/copper-Q5 then passed through a second column with 4 Å sieves. All solvents were stored over 4 Å molecular sieves for 24 hours prior to use. $SnCl_4$ (99%) and PMe_3 (98%) were purchased from Aldrich and used as received. $AlCl_3$ was purchased from Aldrich and sublimed prior to use.

Solution ^{1}H, ^{13}C, ^{31}P and ^{119}Sn NMR spectra were collected at the indicated temperature on the Bruker Avance 500 NMR spectrometer. Chemical shifts are reported in ppm relative to an external reference standard [100% $SiMe_4$ (^{1}H, ^{13}C), 85% H_3PO_4 (^{31}P), and 90% $SnMe_4$ (^{119}Sn)]. NMR spectra of reaction mixtures were obtained by transferring an aliquot of the bulk solution to a 5mm NMR tube. Tubes were then capped tightly and covered with parafilm and Teflon tape.

The ^{31}P CP/MAS NMR experiments were carried out on a Bruker DSX Avance NMR spectrometer with a 9.4T magnet (400.2 MHz proton Larmor frequency, 162.02 MHz ^{31}P Larmor frequency) using a probe head for rotors of 4 mm diameter. The samples were spun at 5.0 kHz, 9.0 kHz and 11.0 kHz to determine center bands and to identify spinning sidebands. Relaxation times for the ^{1}H NMR experiments were determined by inversion recovery sequences. From these experiments recycle delays between 4 and 12 seconds for the ^{31}P cross-polarization (CP) / magic angle spinning (MAS) were determined. The other parameters for the ^{31}P CP/MAS experiments with TPPM proton decoupling were optimized on $NH_4H_2PO_4$, whose resonance also served as external, secondary chemical shift standard at 0.81 ppm. For the CP/MAS NMR spectrum up to 32 scans were accumulated, using 500 micro seconds CP contact times.

Infrared spectra were collected on samples prepared as nujol mulls between CsI plates using a Bruker Vector FT-IR spectrometer. Raman spectra were collected using a Bruker RFS 100 FT-Raman Spectrometer on samples sealed in 1.5-1.8 mm capillaries under dry nitrogen.

Melting points were obtained on samples in capillaries plugged with silicon grease and Teflon tape, under dry nitrogen, by use of an electrothermal apparatus. All reported values are uncorrected. Elemental analyses were performed by Canadian Microanalytical Services Ltd. Delta, British Columbia, Canada. Peaks are reported in wavenumbers (cm^{-1}) with relative intensities (strong[s], medium[m], weak[w]) in parentheses.

Unless otherwise stated, slow evaporation at an indicated temperature was used to isolate X-ray quality crystals. After deposition of crystals, the solvent was carefully removed using a pipette and the crystals were coated with n-paratone oil. Single crystal X-ray diffraction data was collected using a Bruker AXS P4/SMART 1000 diffractometer. All measurements were made with graphite monochromatic Mo-Kα radiation (0.71073 Å). The data was reduced (SAINT)[1] and corrected for absorption (SADABS)[2] and were corrected for Lorentz and polarization effects. The structures were solved by direct methods and expanded using Fourier techniques. Full matrix least squares refinement was carried out on F2 data using the program SHELX97. All crystallographic data collection and refinement was performed by Dr. Andreas Decken at the University of New Brunswick.

Preparation of $SnCl_4(PMe_3)_2$

PMe_3 (761 mg, 10 mmol) in CH_2Cl_2 (16 mL) was added dropwise to $SnCl_4$ (1.302 g, 5 mmol) stirring in CH_2Cl_2 (14 mL). After 1 hour the colorless, opaque reaction mixture was concentrated producing colorless powder, the remaining solvent was decanted off and the colorless powder was dried in *vaccuo*. Crystalline material was obtained by dissolving the slightly-soluble powder in CH_2Cl_2 (20 mL) from which the colorless supernatant was decanted and allowed to slowly evaporate over 6 days at room temperature; this yielded colorless single crystals suitable X-ray diffraction experiments, the crystals were washed with hexane (3 x 7 mL) and dried *in vacuo*.

Yield: 1.782 g (4.33 mmol, 86%, powder), 0.388 g (0.94 mmol, 19%, crystalline)

M.p. 201-204°C (powder), 202-204°C (crystalline)

E.A. calculated (actual) of crystals: C 17.46% (17.32%), H 4.40% (4.49%)

FT-IR (nujol mull on KBr plates, cm^{-1}, [relative intensities]): 2960[s], 2924[bs], 2871[s], 2854[s], 1465[s], 1460[s], 1394[m], 1376[m], 1293[w], 1250[m], 1209[w], 1199[w], 1158[m], 1091[m], 1056[m], 1034[m], 928[w], 881[m], 790[s], 681[m], 659[m], 598[w], 536 [m], 494 [bs]

FT-Raman (capillary tube - 1mm, cm^{-1}, [relative intensities]): 2985[m], 2910[s], 1403[w], 764[w], 664[w], 349[w], 334[w], 289[w], 228[w], 267[w], 174[w]

^{1}H NMR (500.1 MHz, CD_2Cl_2, 295K): δ 1.80-1.83 ppm (18H, *m*, P[CH_3]$_3$)

^{13}C{^{1}H} NMR (125.8 MHz, CD_2Cl_2, 295K): δ 10.15-10.39 ppm (*m*, P[CH$_3$]$_3$)

^{31}P{^{1}H} NMR (202.5 MHz, CD_2Cl_2, 295K): δ 1.6 ppm (*s*), tin satellittes present (*d*, $^{1}J_{P\text{-}119Sn}$ = 2635 Hz, $^{1}J_{P\text{-}117Sn}$ = 2517 Hz)

^{119}Sn NMR (186.5 MHz, CD_2Cl_2, 295K): δ -554 ppm (*t*, $^{1}J_{PSn}$ = 2635 Hz)

^{31}P CP/MAS (62.02 MHz, 4mm rotor, 9.0 kHz spinning, 295K): 6.74 ppm (*s*) tin satellites present but not distinguishable (*d*, $^{1}J_{PSn}$ = 2772 Hz)

Crystal Data: See Table **S1**

Preparation of $[SnCl_3(PMe_3)_2][AlCl_4]$

PMe_3 (761 mg, 10 mmol) in CH_2Cl_2 (13 mL) was added rapidly to a stirring mixture of $AlCl_3$ (667 mg, 5 mmol) and $SnCl_4$ (1.302 g, 5 mmol) in CH_2Cl_2 (32 mL). After 1 hour the pale yellow, opaque reaction mixture was concentrated producing off-white powder. Remaining solvents were decanted and the off-white powder was dried in *vacuo*. Crystalline material was obtained by dissolving the slightly-soluble powder in CH_2Cl_2 (20 mL) from which the pale yellow supernatant was decanted and allowed to slowly evaporate over 6 days at room temperature; this yielded colorless single crystals suitable X-ray diffraction experiments, the crystals were washed with hexane (3 x 7 mL) and dried *in vacuo*.

Yield: 2.482 g (4.56 mmol, 91%, powder), 0.772 g (1.42 mmol, 28%, crystalline)

M.p. 171-175°C (powder), 172-175°C (crystalline)

E.A. calculated (actual) of crystals: C 13.36% (13.20%), H 3.32% (3.32%)

FT-IR (nujol mull on KBr plates, cm^{-1}, [relative intensities]): 2955[s], 2924[bs], 2854[s], 1458[bm], 1422[m], 1410[s], 1377[m], 1304[w], 1295[m], 1288[m], 1268[w], 1010[w], 960[bs], 851[w], 842[w], 829[w], 759[m], 722[w], 664[w], 528[m], 495[s], 488[s], 444[w]

FT-Raman (capillary tube - 1mm, cm^{-1}, [relative intensities]): 2985[m], 2905[s], 1401[w], 759[w], 668[w], 338[w], 321[w], 309[w], 268[ms], 234[w], 201[w], 178[w]

^{1}H NMR (500.1 MHz, CD_2Cl_2, 295K): δ 1.93-1.96 ppm (18H, *m*, P[C*H*$_3$]$_3$)

^{13}C{^{1}H} NMR (125.8 MHz, CD_2Cl_2, 295K): δ 10.14-10.39 ppm (*m*, P[*C*H$_3$]$_3$)

^{31}P{^{1}H} NMR (202.5 MHz, CD_2Cl_2, 295K): δ 10.8 ppm (*s*), tin satellites present (*d*, $^{1}J_{P\text{-}119Sn}$ = 2725 Hz, $^{1}J_{P\text{-}117Sn}$ = 2604 Hz)

^{119}Sn NMR (186.5 MHz, CD_2Cl_2, 295K): δ -456 ppm (*t*, $^{1}J_{PSn}$ = 2725 Hz)

^{31}P CP/MAS (62.02 MHz, 4mm rotor, 9.0 kHz spinning, 295K): 15.9 ppm (*s*) tin satellites present but not distinguishable (*d*, $^{1}J_{PSn}$ = 2706 Hz)

Crystal Data: See Table **S1**

Preparation of $[SnCl_2(PMe_3)_2][AlCl_4]_2$

PMe_3 (761 mg, 10 mmol) in CH_2Cl_2 (16 mL) was added rapidly to a stirring mixture of $AlCl_3$ (1.333 g, 10 mmol) and $SnCl_4$ (1.302 g, 5 mmol) in CH_2Cl_2 (16 mL). After 2 hours the yellow, opaque reaction mixture was allowed to separate revealing colorless precipitate with yellow, clear supernatant. Crystalline material was obtained by decanting the yellow, clear supernatant which was left to slowly evaporate over 6 days at room temperature; this yielded

colorless single crystals suitable X-ray diffraction experiments, the crystals were washed with hexane (3 x 7 mL) and dried *in vacuo*.

Yield: 3.289 g (4.82 mmol, 96%, powder), 0.250 g (0.37 mmol, 7%, crystalline)

D.p./m.p. 155–157 °C (decomposition occurs to produce a colorless solid which then melts at 233-235 °C).

E.A. calculated (actual) of crystals: C 10.61% (10.54%), H 2.67% (2.64%)

FT-IR (nujol mull on CsI plates, cm^{-1}, [relative intensities]): 2956[s], 2921[bs], 2854[s], 1462[bm], 1418[m], 1403[s], 1377[m], 1311[w], 1296[s], 960[s], 947[s], 853[w], 762[s], 722[w], 664[s], 526[bs], 428[s]

FT-Raman (capillary tube - 1mm, cm^{-1}, [relative intensities]): 2996[m], 2981[m], 2919[ms], 2907[s], 1399[w], 763[w], 667[w], 360[w], 329[m], 193[w], 174[m]

^{1}H NMR (500.1 MHz, CD_2Cl_2, 295K): δ 2.05-2.08 ppm (18H, *m*, P[CH_3]$_3$)

^{13}C{^{1}H} NMR (125.8 MHz, CD_2Cl_2, 295K): δ 9.96-10.21 ppm (*m*, P[CH$_3$]$_3$)

^{31}P{^{1}H} NMR (202.5 MHz, CD_2Cl_2, 295K): δ 16.9 ppm (*s*), tin satellites present (*d*, $^{1}J_{P\text{-}119Sn}$ = 2591 Hz, $^{1}J_{P\text{-}117Sn}$ = 2476 Hz)

^{119}Sn NMR (186.5 MHz, CD_2Cl_2, 295K):): δ -333 ppm (*t*, $^{1}J_{PSn}$ = 2591 Hz)

^{31}P CP/MAS (62.02 MHz, 4mm rotor, 9.0 kHz spinning, 295K): 46.3 ppm (*s*) tin satellites present but not distinguishable (*d*, $^{1}J_{PSn}$ = 2125 Hz); 45.8 ppm (*s*) tin satellites present but not distinguishable (*d*, $^{1}J_{PSn}$ = 2125 Hz)

Crystal Data: see Table S**1**

^{31}P Solution and CP/MAS NMR Discussion:

Chemical shifts in the $^{31}P\{^{1}H\}$ solution NMR of neutral, mono- and dication are observed in a narrow range, while the $^{119}Sn\{^{1}H\}$ NMR data exhibits a substantial deshielding with increased charge. ^{31}P CP/MAS NMR data (Figure S1) are consistent with solution data within 5 ppm. The relatively large chemical shift of 28 ppm between solution and CP/MAS data for $[(Me_3P)_2SnCl_2][AlCl_4]_2$ is likely due to the solvent interactions being distinct from those involving the aluminate counter ions in the solid-state. In addition, the two signals of equal intensity observed in the CP/MAS of $[(Me_3P)_2SnCl_2][AlCl_4]_2$ shows at 46.3 and 45.8 ppm are attributed to crystallographically distinct PMe_3 groups.

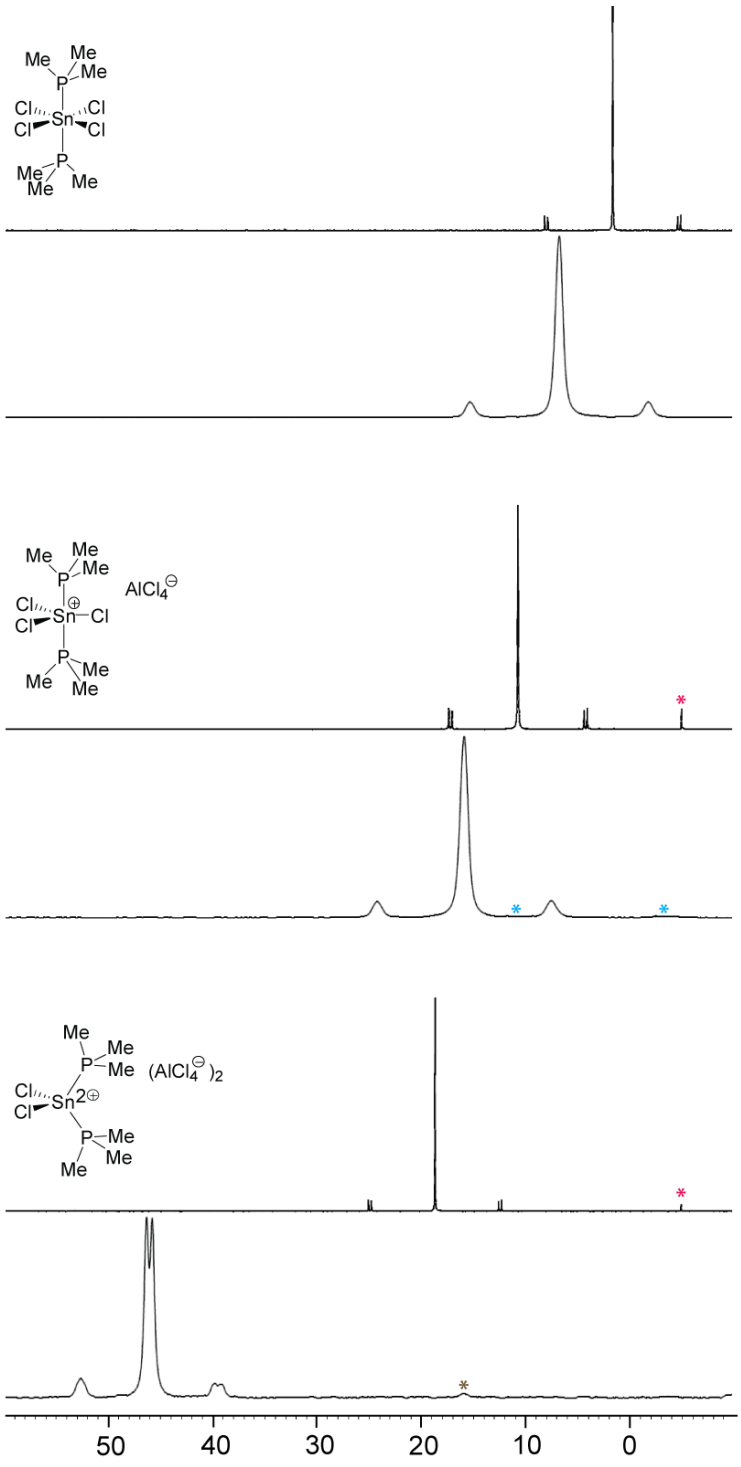

Figure S1: Solution $^{31}P\{^{1}H\}$ NMR (above) and solid-state ^{31}P CP/MAS NMR (below) spectra for compounds $SnCl_4(PMe_3)_2$, $[SnCl_3(PMe_3)_2][AlCl_4]$ and $[SnCl_2(PMe_3)_2][AlCl_4]_2$. Signals assigned to a $[Me_3PH]^+$ impurity are labeled with red asterisks, signals assigned to unknown side products are labeled with blue asterisks and $[(PMe_3)_2SnCl_3][AlCl_4]$ impurity is labeled with a brown asterisk.

Single Crystal X-Ray Data:

Table S1: Selected crystallographic data for $SnCl_4(PMe_3)_2$, $[SnCl_3(PMe_3)_2][AlCl_4]$ and $[SnCl_2(PMe_3)_2][AlCl_4]_2$.

	$SnCl_4(PMe_3)_2$	$[SnCl_3(PMe_3)_2][AlCl_4]$	$[SnCl_2(PMe_3)_2][AlCl_4]_2$
Empirical formula	$C_6H_{18}Cl_4P_2Sn$	$C_6H_{18}AlCl_7P_2Sn$	$C_6H_{18}Al_2Cl_{10}P_2Sn$
Fw	412.63	545.96	679.29
T (K)	188(1)	198(1)	188(1)
λ(Mo Kα) (Å)	0.71073	0.71073	0.71073
color and habit	Colorless, irregular	Colorless, irregular	Colorless, plate
cryst syst	Monoclinic	Monoclinic	Monoclinic
space group	$P2_1/c$	$P2_1/c$	$P2_1/n$
a (Å)	6.6923(14)	9.164(3)	7.2631(8)
b (Å)	8.4333(17)	10.897(3)	13.2705(14)
c (Å)	13.376(3)	10.684(3)	25.978(3)
α (deg)	90	90	90
β (deg)	100.204(2)	105.708(3)	95.048(2)
γ (deg)	90	90	90
V ($Å^3$)	743.0(3)	1027.1(5)	2494.2(5)
Z	2	2	4
cryst size (mm^3)	0.25 x 0.10 x 0.10	0.35 x 0.35 x 0.15	0.30 x 0.15 x 0.05
abs coeff (mm^{-1})	2.617	2.334	2.285
reflens colled	3093	7106	17052
indpndt reflens	1656	2430	5570
R_{int}	0.0315	0.0248	0.0574
θ_{max} (deg)	27.49	27.50	27.50
GoF	1.033	1.069	1.052
R1(all data)	0.0311	0.0262	0.0921
wR2 (all data)	0.0573	0.0674	0.1083
largest diff peak and hole (e $Å^{-3}$)	0.551 and -0.474	0.871 and -0.701	1.340 and -0.924
CCDC	885483	885484	885485

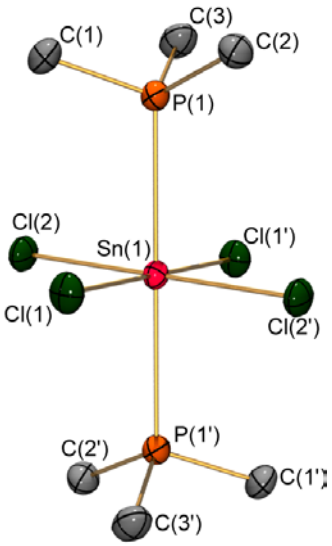

Figure S2: POV-Ray view of the molecular structure of $SnCl_4(PMe_3)_2$. Thermal ellipsoids are at the 50% probability level and hydrogen atoms are omitted for clarity.

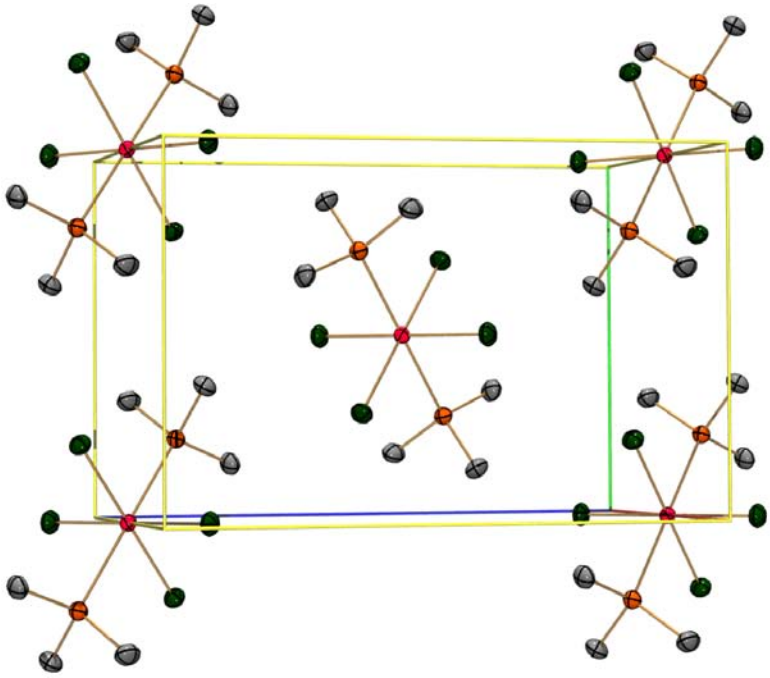

Figure S3: POV-Ray view of the unit cell contents of $SnCl_4(PMe_3)_2$. Thermal ellipsoids are at the 50% probability level and hydrogen atoms are omitted for clarity.

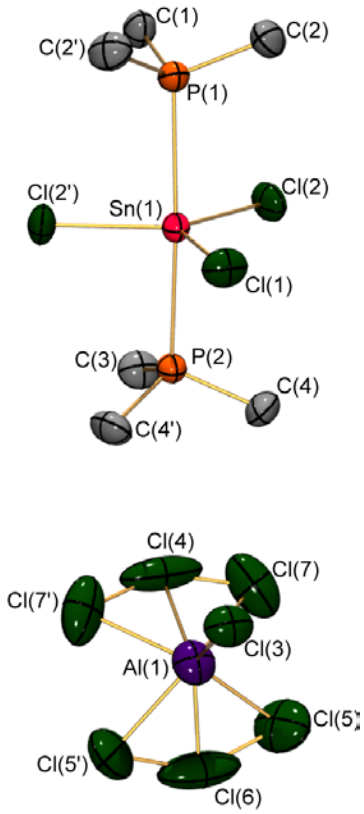

Figure S4: POV-Ray view of the molecular structure of the cation $[(PMe_3)_2][AlCl_4]$. Thermal ellipsoids are at the 50% probability level and hydrogen atoms are omitted for clarity.

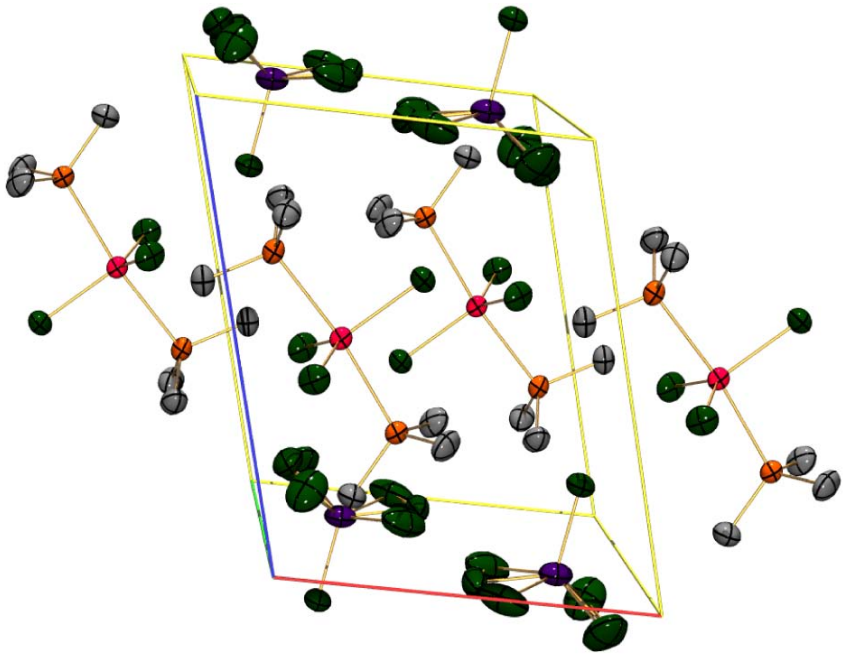

Figure S5: POV-Ray view of the unit cell contents of $[(PMe_3)_2][AlCl_4]$. Thermal ellipsoids are at the 50% probability level and hydrogen atoms are omitted for clarity.

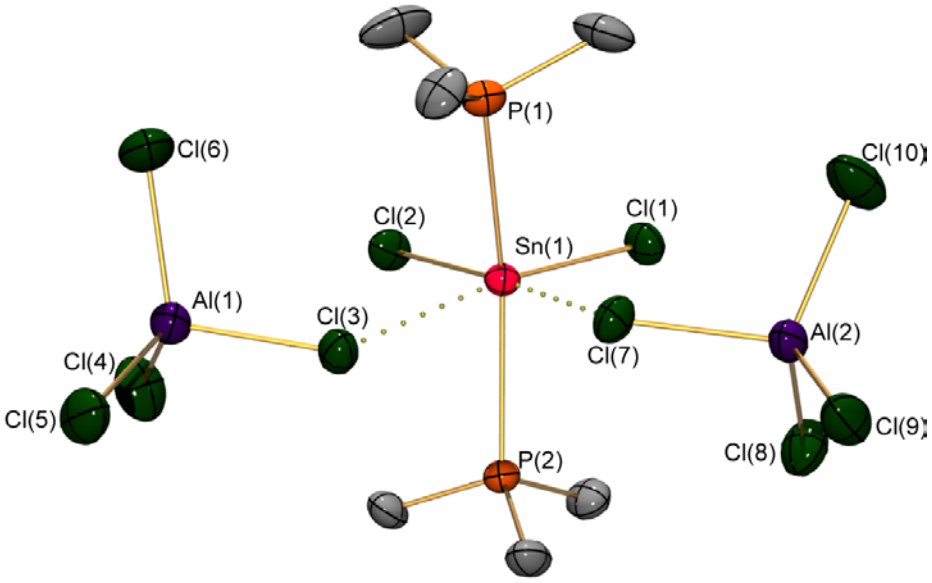

Figure S6: POV-ray view of the molecular structure of $[SnCl_2(PMe_3)_2][AlCl_4]_2$, thermal ellipsoids are drawn at the 50% probability level and hydrogen atoms are omitted for clarity.

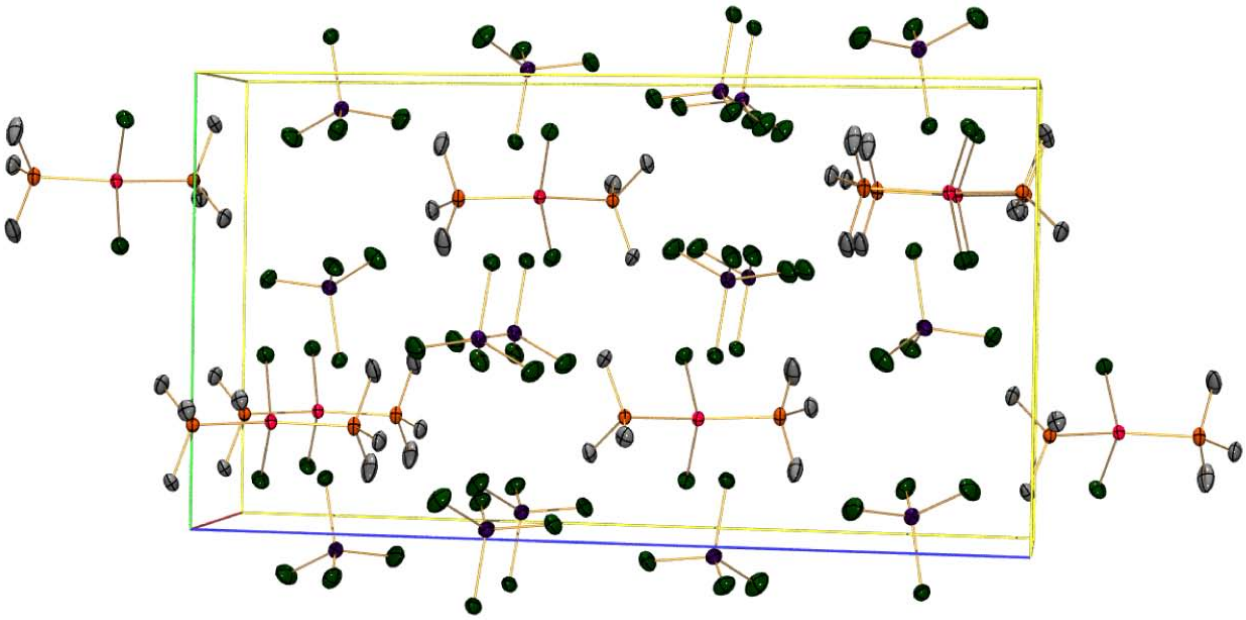

Figure S7: POV-Ray view of the unit cell contents of $[SnCl_2(PMe_3)_2][AlCl_4]_2$, thermal ellipsoids are drawn at the 50% probability level and hydrogen atoms are omitted for clarity.

Table S2: Selected bond lengths (Å) and angles (°) for $SnCl_4(PMe_3)_2$ (atomic numbering scheme shown in Figure S2).

Sn(1)-Cl(2′)	2.4565(7)	Sn(1)-P(1)	2.5654(7)
Sn(1)-Cl(2)	2.4565(7)	P(1)-C(3)	1.798(2)
Sn(1)-Cl(1′)	2.4762(6)	P(1)-C(1)	1.798(2)
Sn(1)-Cl(1)	2.4762(6)	P(1)-C(2)	1.804(2)
Sn(1)-P(1′)	2.5654(7)		
Cl(2′)-Sn(1)-Cl(2)	180.0	Cl(2)-Sn(1)-P(1)	92.00(2)
Cl(2′)-Sn(1)-Cl(1′)	89.47(2)	Cl(1′)-Sn(1)-P(1)	92.78(2)
Cl(2)-Sn(1)-Cl(1′)	90.53(2)	Cl(1)-Sn(1)-P(1)	87.22(2)
Cl(2′)-Sn(1)-Cl(1)	90.53(2)	P(1′)-Sn(1)-P(1)	180.0
Cl(2)-Sn(1)-Cl(1)	89.47(2)	C(3)-P(1)-C(1)	108.01(12)
Cl(1′)-Sn(1)-Cl(1)	180.00(2)	C(3)-P(1)-C(2)	106.92(12)
Cl(2′)-Sn(1)-P(1′)	92.00(2)	C(1)-P(1)-C(2)	107.46(11)
Cl(2)-Sn(1)-P(1′)	88.00(2)	C(3)-P(1)-Sn(1)	111.97(8)
Cl(1′)-Sn(1)-P(1′)	87.22(2)	C(1)-P(1)-Sn(1)	112.98(8)
Cl(1)-Sn(1)-P(1′)	92.78(2)	C(2)-P(1)-Sn(1)	109.23(8)
Cl(2′)-Sn(1)-P(1)	88.00(2)		

Table S3: Selected bond lengths (Å) and angles (°) for $[SnCl_3(PMe_3)_2][AlCl_4]$ (atomic numbering scheme shown in Figure S4).

Sn(1)-Cl(1)	2.3490(12)	P(2)-C(4′)	1.790(3)
Sn(1)-Cl(2)	2.3955(10)	P(2)-C(4)	1.790(3)
Sn(1)-Cl(2′)	2.3955(10)	Al(1)-Cl(6)	1.908(4)
Sn(1)-P(2)	2.5347(12)	Al(1)-Cl(4)	1.981(3)
Sn(1)-P(1)	2.5439(12)	Al(1)-Cl(3)	2.130(2)
P(1)-C(1)	1.791(5)	Al(1)-Cl(5)	2.180(3)
P(1)-C(2′)	1.791(4)	Al(1)-Cl(5′)	2.180(3)
P(1)-C(2)	1.791(4)	Al(1)-Cl(7)	2.246(4)
P(2)-C(3)	1.788(5)	Al(1)-Cl(7′)	2.246(4)
Cl(1)-Sn(1)-Cl(2)	113.49(2)	Cl(6)-Al(1)-Cl(4)	130.27(18)
Cl(1)-Sn(1)-Cl(2′)	113.49(2)	Cl(6)-Al(1)-Cl(3)	119.04(18)
Cl(2)-Sn(1)-Cl(2′)	133.00(5)	Cl(4)-Al(1)-Cl(3)	110.69(12)
Cl(1)-Sn(1)-P(2)	92.23(4)	Cl(6)-Al(1)-Cl(5)	50.94(9)
Cl(2)-Sn(1)-P(2)	88.54(2)	Cl(4)-Al(1)-Cl(5)	113.81(10)
Cl(2′)-Sn(1)-P(2)	88.54(2)	Cl(3)-Al(1)-Cl(5)	108.06(10)
Cl(1)-Sn(1)-P(1)	95.10(5)	Cl(6)-Al(1)-Cl(5′)	50.94(9)
Cl(2)-Sn(1)-P(1)	88.54(3)	Cl(4)-Al(1)-Cl(5′)	113.81(10)
Cl(2′)-Sn(1)-P(1)	88.54(3)	Cl(3)-Al(1)-Cl(5′)	108.06(11)
P(2)-Sn(1)-P(1)	172.67(4)	Cl(5)-Al(1)-Cl(5′)	101.89(18)
C(1)-P(1)-C(2′)	108.92(15)	Cl(6)-Al(1)-Cl(7)	113.90(15)
C(1)-P(1)-C(2)	108.92(15)	Cl(4)-Al(1)-Cl(7)	48.85(13)
C(2′)-P(1)-C(2)	109.4(3)	Cl(3)-Al(1)-Cl(7)	104.91(10)
C(1)-P(1)-Sn(1)	108.00(17)	Cl(5)-Al(1)-Cl(7)	70.64(14)
C(2′)-P(1)-Sn(1)	110.79(12)	Cl(5′)-Al(1)-Cl(7)	146.84(14)
C(2)-P(1)-Sn(1)	110.79(12)	Cl(6)-Al(1)-Cl(7′)	113.90(15)
C(3)-P(2)-C(4)	109.05(16)	Cl(4)-Al(1)-Cl(7′)	48.85(13)
C(3)-P(2)-C(4)	109.05(16)	Cl(3)-Al(1)-Cl(7′)	104.91(10)
C(4′)-P(2)-C(4)	109.1(3)	Cl(5)-Al(1)-Cl(7′)	146.84(14)
C(3)-P(2)-Sn(1)	111.63(18)	Cl(5′)-Al(1)-Cl(7′)	70.64(14)
C(4′)-P(2)-Sn(1)	108.98(13)	Cl(7)-Al(1)-Cl(7′)	97.6(2)
C(4)-P(2)-Sn(1)	108.98(13)		

Table S4: Selected bond lengths (Å) and angles (°) for $[SnCl_2(PMe_3)_2][AlCl_4]_2$ (atomic numbering scheme shown in Figure S6).

Sn(1)-Cl(2)	2.3367(5)	Al(2)-Cl(8)	2.1120(9)
Sn(1)-Cl(1)	2.3575(5)	Al(2)-Cl(9)	2.1166(9)
Sn(1)-P(2)	2.5390(6)	Al(2)-Cl(10)	2.1194(9)
Sn(1)-P(1)	2.5414(6)	Al(2)-Cl(7)	2.1993(8)
Sn(1)-Cl(3)	2.9233(6)	P(1)-C(1)	1.785(2)
Sn(1)-Cl(7)	2.9907(6)	P(1)-C(2)	1.792(2)
Al(1)-Cl(5)	2.1107(9)	P(1)-C(3)	1.796(2)
Al(1)-Cl(6)	2.1164(9)	P(2)-C(4)	1.783(2)
Al(1)-Cl(4)	2.1176(8)	P(2)-C(6)	1.792(2)
Al(1)-Cl(3)	2.2073(8)	P(2)-C(5)	1.793(2)
Cl(2)-Sn(1)-Cl(1)	102.25(2)	Cl(8)-Al(2)-Cl(9)	114.21(4)
Cl(2)-Sn(1)-P(2)	98.825(19)	Cl(8)-Al(2)-Cl(10)	113.06(4)
Cl(1)-Sn(1)-P(2)	95.209(19)	Cl(9)-Al(2)-Cl(10)	109.98(4)
Cl(2)-Sn(1)-P(1)	97.185(19)	Cl(8)-Al(2)-Cl(7)	106.44(3)
Cl(1)-Sn(1)-P(1)	96.654(19)	Cl(9)-Al(2)-Cl(7)	107.20(4)
P(2)-Sn(1)-P(1)	157.554(19)	Cl(10)-Al(2)-Cl(7)	105.33(3)
Cl(2)-Sn(1)-Cl(3)	91.968(19)	Al(1)-Cl(3)-Sn(1)	119.43(3)
Cl(1)-Sn(1)-Cl(3)	165.284(17)	Al(2)-Cl(7)-Sn(1)	127.63(3)
P(2)-Sn(1)-Cl(3)	86.219(18)	C(1)-P(1)-C(2)	109.37(12)
P(1)-Sn(1)-Cl(3)	77.591(17)	C(1)-P(1)-C(3)	108.13(13)
Cl(2)-Sn(1)-Cl(7)	165.882(17)	C(2)-P(1)-C(3)	108.65(15)
Cl(1)-Sn(1)-Cl(7)	91.68(2)	C(1)-P(1)-Sn(1)	116.25(8)
P(2)-Sn(1)-Cl(7)	77.407(17)	C(2)-P(1)-Sn(1)	106.62(8)
P(1)-Sn(1)-Cl(7)	83.254(17)	C(3)-P(1)-Sn(1)	107.61(9)
Cl(3)-Sn(1)-Cl(7)	74.296(17)	C(4)-P(2)-C(6)	109.47(11)
Cl(5)-Al(1)-Cl(6)	112.55(4)	C(4)-P(2)-C(5)	109.11(11)
Cl(5)-Al(1)-Cl(4)	112.68(4)	C(6)-P(2)-C(5)	108.26(11)
Cl(6)-Al(1)-Cl(4)	111.83(4)	C(4)-P(2)-Sn(1)	114.48(8)
Cl(5)-Al(1)-Cl(3)	108.80(4)	C(6)-P(2)-Sn(1)	106.96(8)
Cl(6)-Al(1)-Cl(3)	105.22(3)	C(5)-P(2)-Sn(1)	108.37(7)
Cl(4)-Al(1)-Cl(3)	105.15(3)		

Additional Raman Details

Due to cation-anion peak overlap, unambiguous assignment of vibrational modes in $[(PMe_3)_2SnCl_3][AlCl_4]$ was not possible. The tetrachlorogallate salt of the cation, $[(PMe_3)_2SnCl_3][GaCl_4]$, was therefore prepared in an analogous manner resulting in clear separation of the cation-anion modes. However, $[(PMe_3)_2SnCl_3][GaCl_4]$ was found to be contaminated by a reaction by-product $(PMe_3)_2GaCl_3$, which was confirmed by independently synthesizing the latter by a direct combination of PMe_3 with 0.5 equivalent of $GaCl_3$. The resulting Raman spectra can be seen in Figure S8. Currently, there is only NMR and Raman evidence for the synthesis of $[(PMe_3)_2SnCl_3][GaCl_4]$ and $[(PMe_3)_2SnCl_2][GaCl_4]_2$, isolation and comprehensive characterization of both of these cations will be done in a future report.

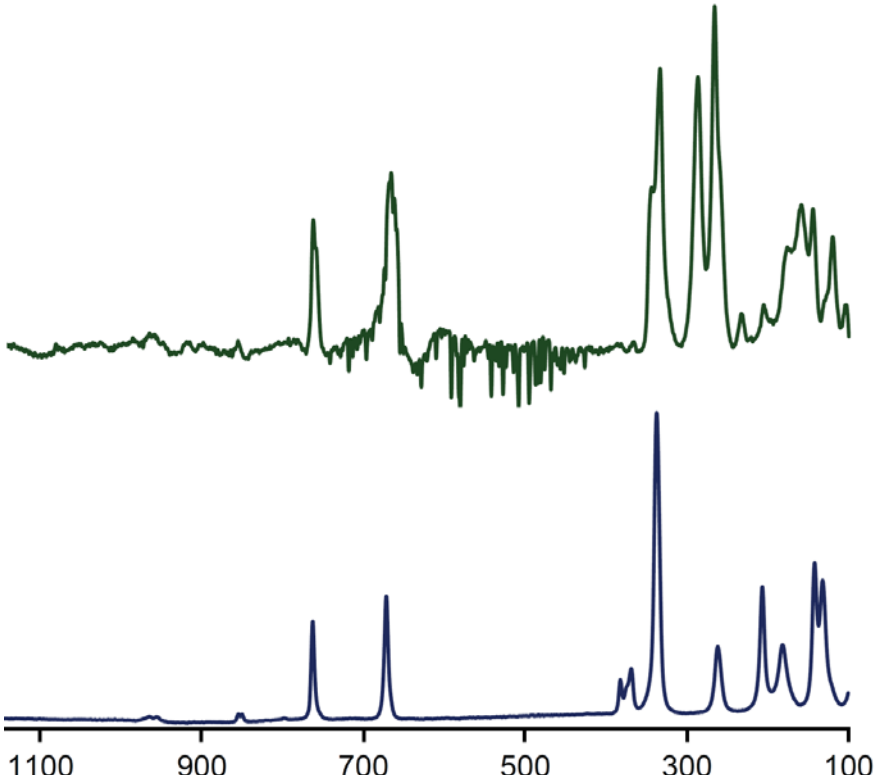

Figure S8: The Raman spectra of $[(PMe_3)_2SnCl_3][GaCl_4]$ (top) and a reaction by-product, $(PMe_3)_2GaCl_3$ (bottom).

Computational Details

The gas-phase structures of $[(PMe_3)_2SnCl_4]$, $[(PMe_3)_2SnCl_3]^+$, and $[(PMe_3)_2SnCl_2]^{2+}$ were optimized using Gaussian09[3] in the absence of any symmetry constraints at the HF and PBE1PBE (PBE0) level[4] which is illustrated in Figure S9 and can be readily compared to the experimental structures in Figure S10. The hybrid basis-set used for all calculations was constructed as follows: SDB-aug-cc-pVTZ[5] + LANL2 ECP[6] for Sn; aug-cc-pVTZ for P and Cl atoms; aug-cc-pVDZ[5] for C and H atoms. The optimized structures were characterized as true minima by frequency calculations at the same level, which produced no imaginary frequencies. The Raman intensities were subsequently calculated to generate Raman spectra for each species using the GaussView03 program. The calculated and observed spectra were overlaid and the relative intensities of the peaks were used as a means of assigning the experimental spectra. The calculated-observed peak pairs thus generated were assigned to a specific vibrational mode by visualizing the atomic displacements of the calculated mode in GaussView03. A representative example of the peak-pairing process is illustrated in Figure S11 for the neutral species. Where ambiguity due to peak overlap with the anion modes was present, a comparison of the Raman spectra of the tetrachloroaluminate and the tetrachlorogallate salts was used to confirm assignments. Figure S12 compares the observed and calculated variations in the average P-Sn, Sn-Cl and P-C bond lengths and the symmetric stretching frequencies. The coordinates of the optimized geometries are listed in Table S5.

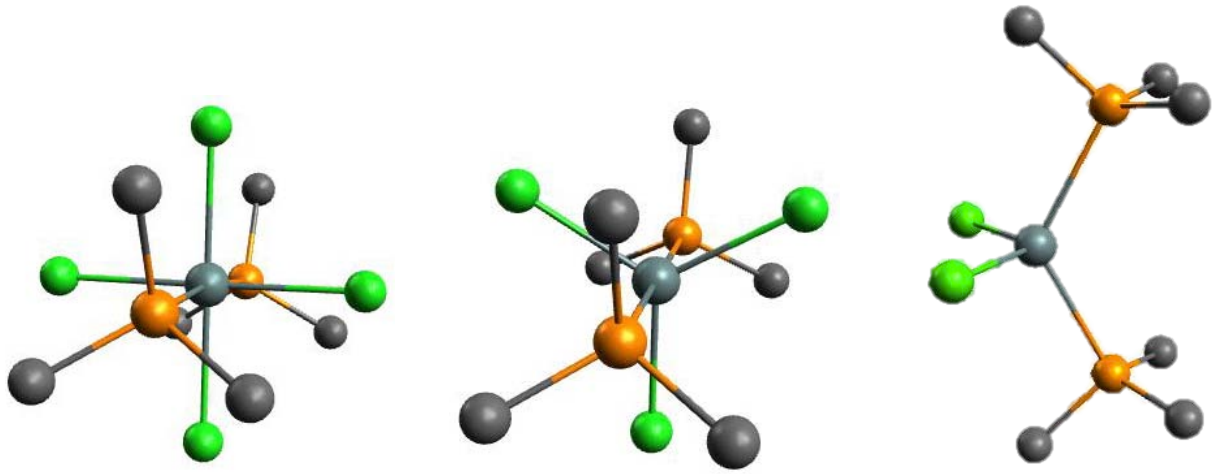

Figure S9: Calculated structures of $[(PMe_3)_2SnCl_4]$ (left, C_{2v}), $[(PMe_3)_2SnCl_3]$ (centre, D_{3h}), and iii) $[(PMe_3)_2SnCl_2]^{2+}$ (right, C_{2v}).

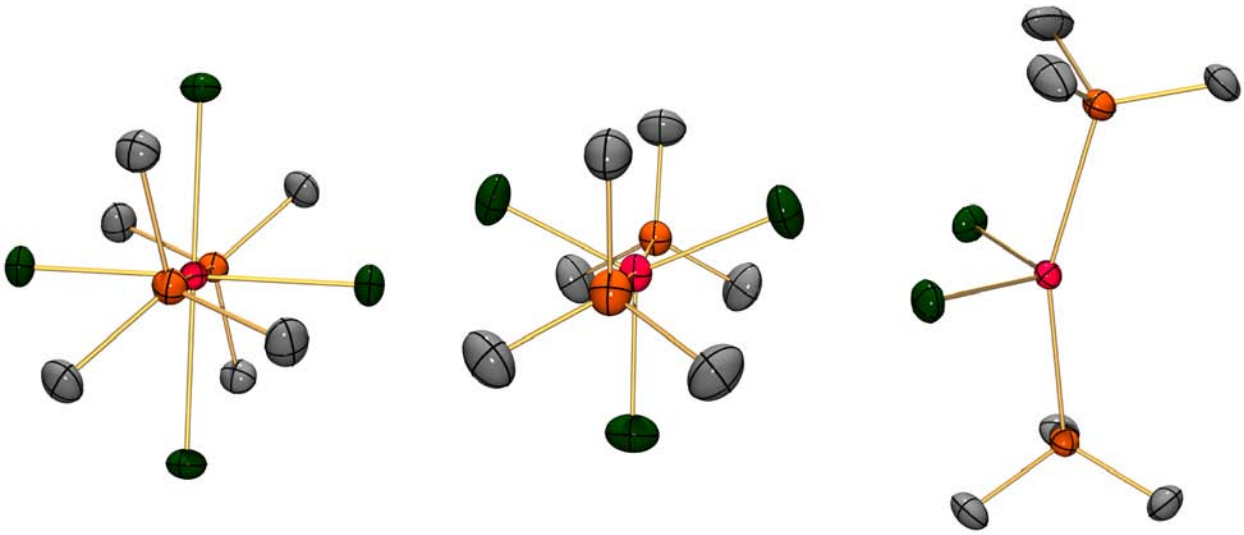

Figure S10: POV-Ray view of the molecular structures of $SnCl_4(PMe_3)_2$ (left), and the cations of $[SnCl_3(PMe_3)_2][AlCl_4]$ (centre) and $[SnCl_2(PMe_3)_2][AlCl_4]_2$ (right). Thermal ellipsoids are at the 50% probability level, hydrogen atoms and counter ions are omitted for clarity.

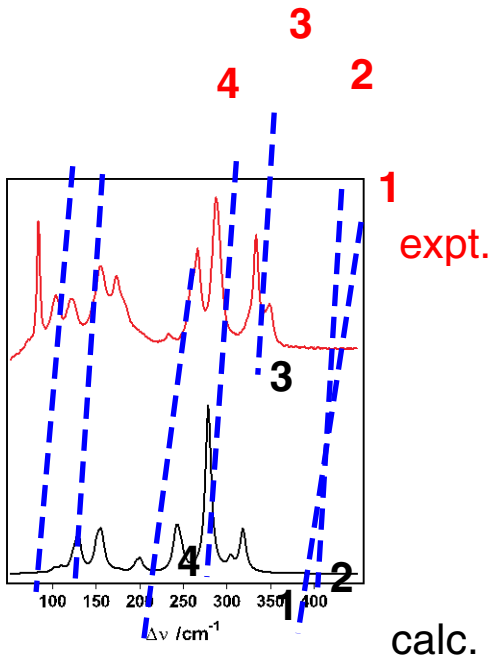

Figure S11: Overlaid experimental and calculated Raman spectra for $[(PMe_3)_2SnCl_4]$ demonstrating the process used for assignment of experimental peaks.

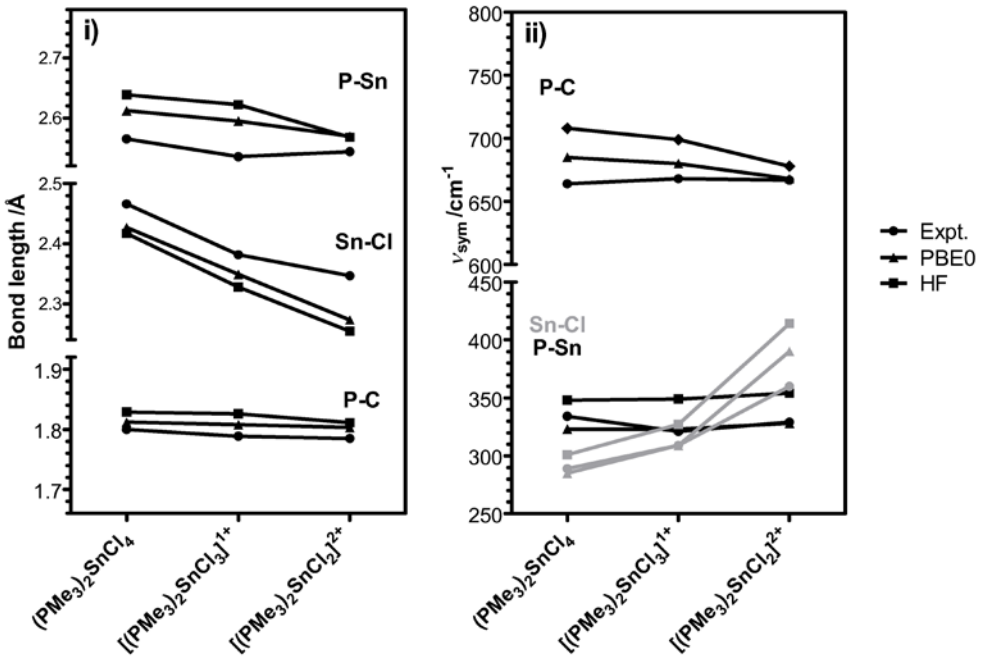

Figure S12: Observed and calculated variations in i) average P-Sn, Sn-Cl and P-C bond lengths (left chart) and ii) symmetric stretching frequencies (right chart).

Table S5: Cartesian coordinates for the optimized geometries of **1**, **2**, and **3** at the HF and PBE1PBE level using the SDB-aug-cc-pVTZ + LANL2ECP basis set on Sn, aug-cc-pVTZ basis set on P, Cl and aug-cc-pVDZ basis set on C and H.

	HF				PBE1PBE			
$[(PMe_3)_2SnCl_4]$	Sn	0.00000	0.06444	-0.00000	Sn	0.00000	0.08264	0.00000
	Cl	-0.00000	0.08506	2.41581	Cl	-0.00000	0.10054	2.42637
	Cl	0.00000	-2.36712	0.00002	Cl	0.00000	-2.36297	0.00001
	Cl	0.00000	0.08502	-2.41581	Cl	0.00000	0.10053	-2.42637
	Cl	0.00000	2.46869	-0.00002	Cl	0.00000	2.49404	-0.00000
	P	2.63777	-0.06012	0.00000	P	2.60751	-0.07504	-0.00000
	P	-2.63777	-0.06012	0.00000	P	-2.60751	-0.07504	-0.00000
	C	3.29714	-0.94568	1.44754	C	3.22987	-0.97218	1.44548
	H	4.38244	-1.03054	1.37043	H	4.32383	-1.07313	1.39294
	H	3.03423	-0.40885	2.35648	H	2.94063	-0.43368	2.35691
	H	2.85517	-1.93953	1.49450	H	2.76074	-1.96497	1.46985
	C	3.45702	1.56542	-0.00001	C	3.43361	1.53793	-0.00002
	H	3.15266	2.12668	0.88192	H	3.11947	2.10223	0.88802
	H	4.54134	1.44185	-0.00001	H	4.52650	1.41424	-0.00002
	H	3.15266	2.12667	-0.88194	H	3.11947	2.10221	-0.88806
	C	3.29714	-0.94570	-1.44752	C	3.22987	-0.97220	-1.44547
	H	3.03423	-0.40888	-2.35647	H	2.94062	-0.43372	-2.35691
	H	4.38245	-1.03056	-1.37041	H	4.32382	-1.07316	-1.39293
	H	2.85517	-1.93955	-1.49447	H	2.76074	-1.96499	-1.46982
	C	-3.45702	1.56542	-0.00001	C	-3.43361	1.53793	-0.00002
	H	-3.15266	2.12667	-0.88195	H	-3.11947	2.10221	-0.88806
	H	-4.54134	1.44185	-0.00001	H	-4.52650	1.41424	-0.00002
	H	-3.15266	2.12668	0.88192	H	-3.11947	2.10223	0.88802
	C	-3.29714	-0.94568	1.44754	C	-3.22987	-0.97218	1.44548
	H	-4.38244	-1.03054	1.37043	H	-4.32383	-1.07313	1.39294
	H	-2.85517	-1.93953	1.49450	H	-2.76074	-1.96497	1.46985
	H	-3.03423	-0.40885	2.35648	H	-2.94064	-0.43368	2.35691
	C	-3.29714	-0.94570	-1.44753	C	-3.22987	-0.97220	-1.44547
	H	-2.85517	-1.93955	-1.49447	H	-2.76073	-1.96500	-1.46982
	H	-4.38244	-1.03056	-1.37042	H	-4.32382	-1.07316	-1.39294
	H	-3.03423	-0.40888	-2.35647	H	-2.94062	-0.43372	-2.35691
$[(PMe_3)_2SnCl_3]^{1+}$	Sn	0.00000	0.00000	0.00000	Sn	0.00000	0.00000	0.00070
	Cl	0.00000	-1.76876	1.51315	Cl	0.00000	0.00000	2.34931
	Cl	0.00000	2.19480	0.77521	Cl	2.03359	0.00000	-1.17425
	Cl	0.00000	-0.42605	-2.28836	Cl	-2.03359	0.00000	-1.17425
	P	-2.62171	0.00000	0.00000	P	0.00000	2.59561	-0.00023
	P	2.62171	0.00000	0.00000	P	0.00000	-2.59561	-0.00023
	C	-3.29695	0.30898	1.65960	C	1.46032	3.24973	0.84228
	H	-4.38690	0.30172	1.62057	H	1.43810	4.34918	0.82849
	H	-2.95873	-0.46511	2.34703	H	1.47305	2.89795	1.88274
	H	-2.95873	1.27861	2.02239	H	2.36741	2.89662	0.33339
	C	-3.29695	-1.59174	-0.56221	C	-1.46032	3.24973	0.84228
	H	-2.95873	-2.39074	0.09612	H	-1.47305	2.89795	1.88274
	H	-4.38690	-1.55432	-0.54899	H	-1.43810	4.34918	0.82849
	H	-2.95874	-1.80003	-1.57632	H	-2.36741	2.89662	0.33339
	C	-3.29695	1.28276	-1.09739	C	0.00000	3.24809	-1.68679
	H	-2.95873	1.11213	-2.11850	H	-0.89450	2.89519	-2.21764
	H	-4.38690	1.25260	-1.07158	H	0.00000	4.34756	-1.66163
	H	-2.95874	2.26515	-0.77072	H	0.89450	2.89519	-2.21764

	C	3.29695	-1.59174	-0.56221	C	-1.46032	-3.24973	0.84228
	H	2.95874	-1.80003	-1.57632	H	-2.36741	-2.89662	0.33339
	H	4.38690	-1.55432	-0.54899	H	-1.43810	-4.34918	0.82849
	H	2.95873	-2.39074	0.09612	H	-1.47305	-2.89795	1.88274
	C	3.29695	0.30898	1.65960	C	1.46032	-3.24973	0.84228
	H	4.38690	0.30172	1.62057	H	1.43810	-4.34918	0.82849
	H	2.95873	1.27861	2.02239	H	2.36741	-2.89662	0.33339
	H	2.95873	-0.46511	2.34703	H	1.47305	-2.89795	1.88274
	C	3.29695	1.28276	-1.09739	C	0.00000	-3.24809	-1.68679
	H	2.95874	2.26515	-0.77072	H	0.89450	-2.89519	-2.21764
	H	4.38690	1.25260	-1.07158	H	0.00000	-4.34756	-1.66163
	H	2.95873	1.11213	-2.11850	H	-0.89450	-2.89519	-2.21764
$[(PMe_3)_2SnCl_3]^{2+}$	Sn	0.00005	0.44792	-0.00020	Sn	0.00000	-0.37929	0.00000
	P	2.25991	-0.77098	0.00068	P	-2.31399	0.73846	-0.00060
	P	-2.25984	-0.77090	-0.00005	P	2.31399	0.73846	0.00060
	C	-2.45858	-1.81943	-1.46647	C	2.59155	1.71188	-1.49110
	H	-3.47070	-2.22810	-1.46174	H	3.64224	2.04327	-1.49225
	H	-2.32022	-1.23093	-2.37341	H	2.41216	1.09762	-2.38494
	H	-1.74834	-2.64483	-1.45091	H	1.94152	2.59726	-1.50903
	C	-3.50882	0.54550	-0.03536	C	3.45277	-0.66051	0.02381
	H	-4.49610	0.07928	-0.03871	H	4.48121	-0.26514	0.02423
	H	-3.41704	1.17902	0.84678	H	3.29933	-1.26441	0.92954
	H	-3.39713	1.15049	-0.93522	H	3.30881	-1.28654	-0.86839
	C	-2.48315	-1.76355	1.50116	C	2.57782	1.74958	1.46961
	H	-3.49574	-2.16601	1.49966	H	3.62815	2.08214	1.47125
	H	-1.78877	-2.58041	1.52399	H	1.92697	2.63447	1.45951
	H	-2.35167	-1.14543	2.38591	H	2.39167	1.15801	2.37724
	C	2.47011	-1.79278	1.48430	C	-2.57782	1.74958	-1.46961
	H	1.75971	-2.61824	1.48938	H	-2.39168	1.15800	-2.37725
	H	3.48210	-2.20153	1.47914	H	-3.62815	2.08214	-1.47126
	H	2.33862	-1.18805	2.38108	H	-1.92697	2.63446	-1.45951
	C	3.50890	0.54583	0.00216	C	-2.59155	1.71188	1.49110
	H	4.49604	0.07977	0.00645	H	-3.64224	2.04327	1.49225
	H	3.41010	1.16311	-0.89056	H	-2.41216	1.09763	2.38494
	H	3.40429	1.16701	0.89145	H	-1.94152	2.59726	1.50902
	C	2.47168	-1.79087	-1.48407	C	-3.45277	-0.66051	-0.02380
	H	2.33288	-1.18681	-2.38050	H	-3.30881	-1.28653	0.86840
	H	3.48654	-2.19277	-1.48262	H	-4.48121	-0.26514	-0.02423
	H	1.76653	-2.62151	-1.48659	H	-3.29933	-1.26441	-0.92953
	Cl	0.00143	1.65760	-1.90263	Cl	0.00242	-1.59982	-1.91700
	Cl	-0.00116	1.65830	1.90183	Cl	-0.00242	-1.59982	1.91700

References:

(1) SAINT 6.02, 1997-1999, Bruker AXS, Inc., Madison, Wisconsin, USA.

(2) SADABS George Sheldrick, 1999, Bruker AXS, Inc., Madison, Wisconsin, USA.

(3) Gaussian 09, Revision A.1, M. J. Frisch, G. W. Trucks, H. B. Schlegel, G. E. Scuseria, M. A. Robb, J. R. Cheeseman, G. Scalmani, V. Barone, B. Mennucci, G. A. Petersson, H. Nakatsuji, M. Caricato, X. Li, H. P. Hratchian, A. F. Izmaylov, J. Bloino, G. Zheng, J. L. Sonnenberg, M. Hada, M. Ehara, K. Toyota, R. Fukuda, J. Hasegawa, M. Ishida, T. Nakajima, Y. Honda, O. Kitao, H. Nakai, T. Vreven, J. A. Montgomery, Jr., J. E. Peralta, F. Ogliaro, M. Bearpark, J. J. Heyd, E. Brothers, K. N. Kudin, V. N. Staroverov, R. Kobayashi, J. Normand, K. Raghavachari, A. Rendell, J. C. Burant, S. S. Iyengar, J. Tomasi, M. Cossi, N. Rega, J. M. Millam, M. Klene, J. E. Knox, J. B. Cross, V. Bakken, C. Adamo, J. Jaramillo, R. Gomperts, R. E. Stratmann, O. Yazyev, A. J. Austin, R. Cammi, C. Pomelli, J. W. Ochterski, R. L. Martin, K. Morokuma, V. G. Zakrzewski, G. A. Voth, P. Salvador, J. J. Dannenberg, S. Dapprich, A. D. Daniels, Ö. Farkas, J. B. Foresman, J. V. Ortiz, J. Cioslowski, and D. J. Fox, Gaussian, Inc., Wallingford CT, 2009.

(4) J. Perdew *et al*, *Phys. Rev. Lett.*, 1996, 77, 3865(E); 1997, 78, 1396.

(5) T. H. Dunning, Jr., *J. Chem. Phys.*, 1989, **90**, 1007.

(6) P. J. Hay and W. R. Wadt, *J. Chem. Phys.*, 1985, **82**, 270; 1985, **82**, 284; 1985, **82**, 299.